The Effect Of Pulsed Electromagnetic Field On The Bone Volume Of Human Being

Yanan Wang[a]*, Wei Zhang[b]

[a]School of Engineering, Deakin University, Geelong, Victoria, 3220, Australia
[b]Department of Metallurgy and Materials, North China University of Science and Technolgy, Qian'An College, Hebei, 064400, China.

Abstract

Pulsed electromagnetic fields (PEMF) devices have been used clinically to slow down osteoporosis and accelerate the healing of bone fractures for many years. However the underlying mechanism by which bone remodeling under PEMF is regulated remains poorly understood. In this paper, a mathematical model of bone cell population of bone remodeling under PEMF at cellular level is developed to address this issue for the first time. Based on this model and control theory, parametric study of control mechanism is carried out and a number of possible control mechanisms are identified. These findings would help further understanding of bone remodeling under PEMF and potential therapies and pharmacological developments in clinical trials.
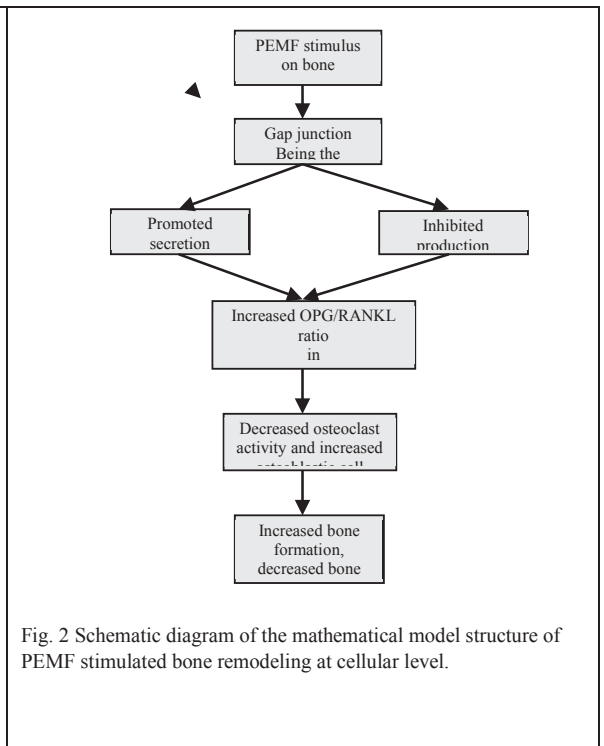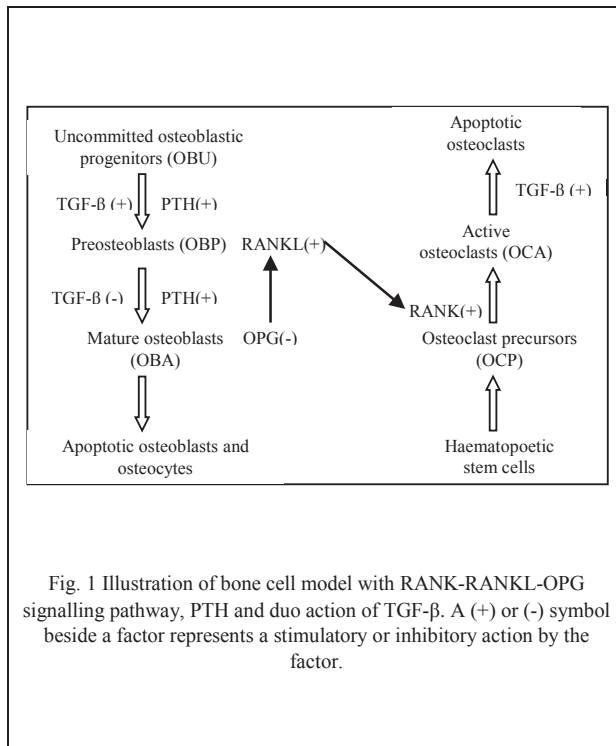
Keywords: bone remodeling; mathematical modelling, pulsed electromagnetic field

1. Introduction

Pulsed electromagnetic fields (PEMF) devices have been widely used clinically for bone healing, muscle relaxation and osteoarthritic joints etc for many years. The osteogenesis effect caused by PEMF device is of great significance to the patients especially who have already undergone failed surgical intervention [1] .

* Corresponding author. School of Engineering, Deakin University, Waurn Ponds campus, Geelong. Tel.: +61 3 5227 3403;
    E-mail address: Yanan.wang@deakin.edu.au

The biological process involved in the osteogenesis of bone caused by PEMF devices is bone remodeling. At cellular level, bone remodeling is an organized process where osteoclasts remove old bone and osteoblasts replace it with newly formed bone. The osteoclasts and osteoblasts work in a coupled manner within a so-called 'basic multicellular unit' (BMU) which is a mediator mechanism bridging individual cellular activity to whole bone morphology [2] and follows an activation-resorption-formation sequence [3]. After the discovery of the RANK-RANKL-OPG pathway [4], there is a clearer picture regarding the control of osteoclastogenesis and bone remodeling in general. The main switch for osteoclastic bone resorption is the RANKL [5], a cytokine that is released by preosteoblasts [6]. Its action on the RANK receptor is regulated by OPG, a decoy receptor, which is also derived from osteoblastic lineage-active osteoblasts [6]. Osteoclast-to-osteoblast cross-talk occurs mostly through growth factors, such as transforming growth factor-β (TGF-β), which are released from the bone matrix during resorption. The RANK-RANKL-OPG signalling pathway between osteoblasts and osteoclasts, TGF-β1, PTH and the dual action of TGF-β is diagrammed in Fig 1.

Fig. 1 Illustration of bone cell model with RANK-RANKL-OPG signalling pathway, PTH and duo action of TGF-β. A (+) or (-) symbol beside a factor represents a stimulatory or inhibitory action by the factor.

Fig. 2 Schematic diagram of the mathematical model structure of PEMF stimulated bone remodeling at cellular level.

Although many in vitro and in vivo studies have been performed, the cellular mechanism by which PEMF affects bone remodeling is still elusive. To the authors' knowledge, no study has been published about this research using mathematical model. To clarify the underlying mechanism at cellular level regulating PEMF's effect on bone remodeling, based on the cell population dynamics model [6] and our previous work [7, 8], the computational system biology method was used with the purpose to understand better bone remodeling under PEMF. Computational system biology uses mathematical modeling to integrate experimental data into a system level model, enabling the various interactions to be efficiently and methodically investigated [9]. The validated model generated by using computational system biology can be used as a tool to reduce ambiguity as to causes and effects in complex systems such as bone remodeling, and makes it possible to test various experimental and theoretical hypotheses "in silico" [10], and more important pharmaceutical and clinical interventions on metabolic bone disease.

2. Mathematical model development

The schematic diagram of the mathematical model structure of bone remodeling under PEMF is illustrated in Fig. 2. In the cell population dynamics model we include three cell populations (see osteoblastic and osteoclastic lineages in Fig. 1) into model equations including osteoblastic precursors (OBP), active osteoblasts (OBA), and active osteoclasts (OCA). Uncommitted osteoblastic progenitors (OBU) and osteoclastic precursors (OCP) are working as reservoirs where the cells will differentiate into functional cells such as osteoblasts and osteoclasts OCP are assigned a very large constant compared with other cell numbers in the model (i.e., OBU= OCP=1×10^{-2} pM).

Similar to [6] and our previous work [7, 8], Hill equation is used to describe the activation and repression of the receptor-ligand interactions. In biochemistry the Hill equation is used to describe the fraction of the macromolecule saturated by a ligand as a function of the ligand concentration; it is used in determining the degree of cooperativity of the ligand binding to the enzyme or receptor. It was originally formulated by Hill in 1910 [11] to describe the sigmoidal O_2 binding curve of haemoglobin:

$$\theta = \frac{L^n}{K_d + L^n} = \frac{L^n}{K_A{}^n + L^n} \tag{1}$$

where θ is the fraction of ligand binding sites filled, L is the ligand concentration, K_d is the apparent dissociation constant derived from the law of mass action, K_A is the ligand concentration producing half occupation and n is the Hill coefficient.

In cell biology, cell responses such as differentiation, proliferation and apoptosis are all related to various ligand–receptor reactions of which some are stimulatory and others are inhibitory [6]. In modeling cell responses, the Hill equation is often used to describe the molecular input function. The activation (act for short) and repression (rep for short) forms of the Hill equation [12] for the production rate of a new cell or molecule are [6]:

$$f\left(x^*\right) = \beta \cdot \Pi_{act} = \frac{\beta x^*}{K_1 + x^*} \tag{2}$$

$$f\left(x^*\right) = \beta \cdot \Pi_{rep} = \frac{\beta}{1 + \dfrac{x^*}{K_2}} \tag{3}$$

where x^* is the active form of concentration x which is a ligand that governs the production of a cell or molecule z through binding to its receptor on cell, β is the maximal production rate of z, and K_1 and K_2 are activation and repression coefficients. Note here that we have already assumed that Hill coefficient equals one.

For convenience, here and later in the paper, we use the abbreviated forms for the factors involved in the corresponding formulation. As in Fig.1 we used OBU for uncommitted osteoblastic progenitors, OBP for osteoblastic precursors, OBA for mature osteoblast, OCP for osteoclast precursor, and OCA for active osteoclasts, also we use RL for RANKL, RK for RANK, Tβ for TGF-β, while OPG and PTH remain unchanged.

The equations governing the evolution of the number of osteoblastic and osteoclastic cells in each maturation stage are simply balance equations [13], which means that each cell stage is fed by an entering flow and is emptied by the outgoing flow of differentiated or apoptotic cells (Fig.1). As a result, utilizing Fig.1 and 2 and based on the formulation in [6], we can formulate the bone cell population dynamics as follows:

$$\frac{dOBP}{dt} = D_{OBU} \cdot OBU \cdot \Pi_{act,OBU}^{T\beta} - D_{OBP} \cdot OBP \cdot \Pi_{rep,OBP}^{T\beta} \tag{4}$$

$$\frac{dOBA}{dt} = D_{OBP} \cdot OBP \cdot \Pi_{rep,OBP}^{T\beta} - A_{OBA} \cdot OBA \tag{5}$$

$$\frac{dOCA}{dt} = D_{OCP} \cdot OCP \cdot \Pi_{act,OCP}^{RL} - A_{OCA} \cdot OCA \cdot \Pi_{act,OCA}^{T\beta} \tag{6}$$

$$\frac{dBV}{dt} = k_{for} \cdot \left[OBA(t) - OBA(t_0) \right] - k_{res} \cdot \left[OCA(t) - OCA(t_0) \right] \tag{7}$$

where subscript 'cell' in the input functions $\Pi_{act/rep,cell}^{molecule}$ means the cell type that a specific molecule binds to and 'molecule' denotes the ligand involved in a particular cell response. D_{OBU} is the differentiation rate of uncommitted OB progenitors, D_{OBP} is the differentiation rate of osteoblastic precursors, D_{OCP} is the differentiation rate of preosteoclasts, A_{OBA} is the rate of elimination of OBA, A_{OCA} is the rate of elimination of OCA. BV stands for bone volume in percentage (%), k_{for} and k_{res} are the relative bone formation and bone resorption rates respectively. We start the simulation from a so-called 'steady-state' where BV is 100%, $dBV/dt = 0$, correspondingly, $OBA(t)$ is $OBA(t_0)$ and $OCA(t)$ is $OCA(t_0)$, as detailed in Appendix A. All the constants and their values can be found in Appendix B.

3. Results and analysis

Bone remodeling is an important biological system when it comes to fracture bone healing, non-union fracture and bone diseases such as osteoporosis etc. It is executed by coordinated activities of osteoclastic cells and osteoblastic cells in BMUs. The coupling between osteoclastic cells and osteoblastic cells is facilitated by the RANK-RANKL-OPG pathway, together with the systemic hormone PTH and transforming growth factor TGF-β. PEMF devices are used clinically to promote bone healing especially non-union fracture but relatively little is known about the mechanisms involved. In this paper we proposed a mathematical model to simulate the PEMF's effect on bone remodeling at cellular level, which would help us understand better about the underlying mechanisms. Here we solved the ordinary differential equations (4)-(7) numerically using Matlab and plotted a series of graphs about the concentration dynamics of OPG, RANKL, cell populations of OBA, OCA and OBP, and bone volume, as can be seen from Fig. 3-Fig. 6, respectively. Note that the parameter values are from the models that this model is based on [6] and our previous work [7, 8]. The effects of PEMF on bone remodeling are characterized by its intensity, frequency, waveform, application time etc, and according to the study [14], the timing of PEMF stimulation does not affect the bone cell development, which is different from the bone remodeling under mechanical stimulus. And in this numerical investigation the specific parameter values of PEMF were chosen from the widely used PEMF devices in clinics [15] and this set of parameter values is the only one used in our model. Consequently we assume that the PEMF'effects on bone remodeling specifically OPG or RANKL in our model do not change (represented by two different constants and   in the model) all the way through the simulation (three months).

The concentration dynamics of OPG during three-month PEMF application is simulated in Fig. 3. Consistent with experimental observations, the OPG concentration increases during the first ten days simulation. Surprisingly the concentration of OPG keeps dropping from the 10th day in simulation. For the reason that most in vitro experiments were done within two weeks, there is no available experimental data to compare with. While the pattern of the OPG concentration might be explained that because of the PEMF's stimulus effect, OPG concentration goes up in the short period after the PEMF's application, then the binding of OPG with RANKL catches up as the bone remodeling occurs, more OPG are consumed than produced by osteoblast cells, as a result, OPG concentration drops till the end of simulation.

Fig. 4 shows the RANKL concentration dynamics during the three-month PEMF application. As can be seen from the graph, within two weeks (which is the time scale of most in vitro experiments), the RANKL concentration drops,

compared with the initial value. However it is not expect that the RANKL concentration increases significantly immediately after the simulation begins, while followed by dramatic decrease afterwards and continue the similar level through the rest of the simulation.
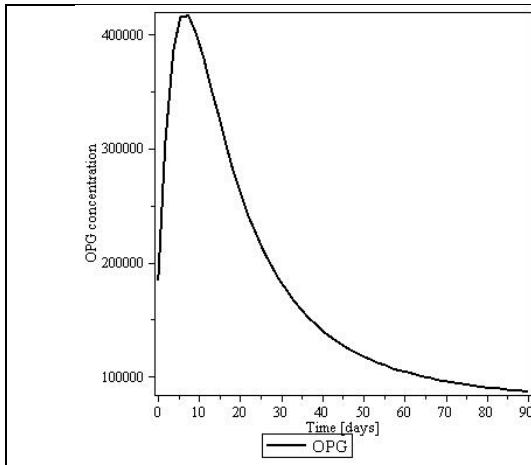

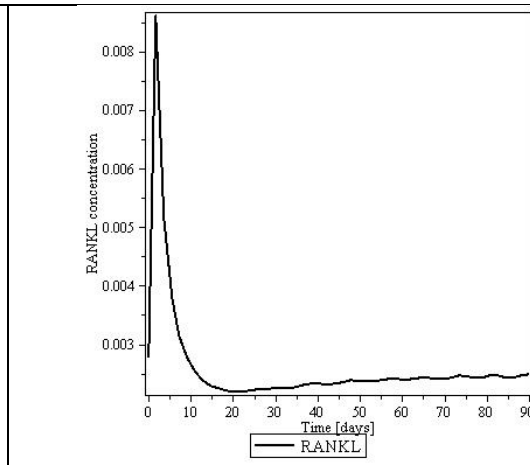Fig. 3 OPG concentration dynamics during three-month PEMF application

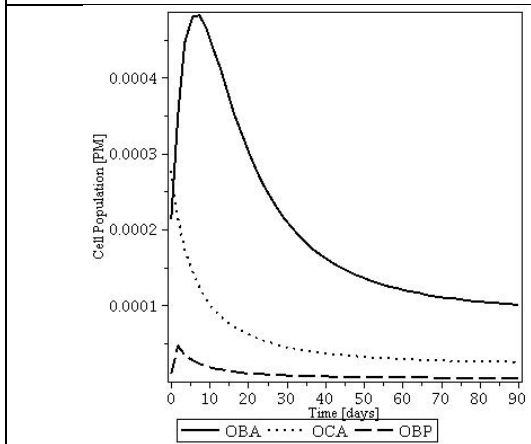Fig. 4 RANKL concentration dynamics during three-month application

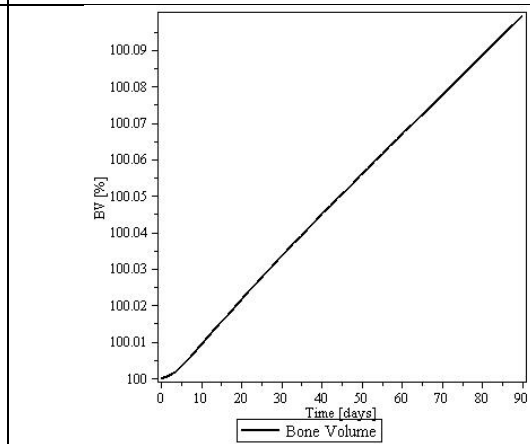Fig. 5 OBA, OCA and OBP cell population dynamics during three-month PEMF application

Fig. 6 Bone volume percentage dynamics during three-month PEMF application

Possible reason for this development pattern is that the number of preosteoblast cells that produce RANKL is increased by the PEMF's stimulus effect on the proliferation of bone marrow mesenchymal stem cells [16] immediately after the application of PEMF, then the inhibitory effect of PEMF on the OBP takes over and this overall trend keeps this way till the end of simulation.

The cell population dynamics of OBA, OCA and OBP can be found in Fig. 5. As expected the OBA and OBP populations rise and OCA goes down in the beginning two weeks of the simulation, which is consistent with experimental observations. Because of the coupling effect between OCA and OBA, the OBA population starts to drop

after it peaks and continues to decrease till the end of simulation while maintaining a higher concentration than OCA which accounts for the continuing growth of bone volume in Fig. 6.

4. Summary and conclusion

In this paper, a mathematical model of bone remodeling under PEMF at cellular level was proposed based on experimental results and our previous work. This model incorporates the latest experimental findings through extensive literature review and summarizes that PEMF applies its physiological effects via RANK-RANKL-OPG pathway, specifically PEMF promotes the secretion of OPG and inhibits the production of RANKL, which overall suppresses the population of osteoclasts that absorb bone minerals. Based on this model, the numerical investigation demonstrates the concentration dynamics of growth factors OPG and cytokines RANKL, and the population dynamics of OBA, OBP and OCA. More importantly, parametric study of bone remodeling under PEMF was carried out in order to understand the control mechanism of bone remodeling at cellular level under PEMF. From a control mechanism perspective, it is quite likely that there are several control mechanisms working simultaneously in bone remodeling which is a complex system. Consequently, we perform an extensive parametric study investigating model parameter space related to cell differentiation and apoptosis which describes the fundamental cell lineage behaviors, to investigate such a scenario. After analyzing all the combinations (that is 242 permutations) of five model parameters, we successfully identified a small number of parameter combinations that are able to cause physiologically realistic responses which are similar to theoretically idealized physiological response. In the end, this work will further our understanding on bone remodeling under PEMF and the identified control mechanisms are able to help to develop combined pharmacological and PEMF therapies to cure bone loss diseases such as osteoporosis.

References

[1] Gossling, R. H, Bernstein, A. R, Abbott, and J, Treatment of ununited tibial fractures : a comparison of surgery and pulsed electromagnetic fields (PEMF) vol. 15. Thorofare, NJ, ETATS-UNIS: Slack, 1992.
[2] H. M. Frost, Intermediary organization of the skeleton: Boca Raton, Fla. : CRC Press, 1986.
[3] A. G. Robling, A. B. Castillo, and C. H. Turner, "Biomechanical and molecular regulation of bone remodeling," Annual Reviews, vol. 8, pp. 455-498, 2006.
[4] D. M. Anderson, E. Maraskovsky, W. L. Billingsley, W. C. Dougall, M. E. Tometsko, E. R. Roux, et al., "A homologue of the TNF receptor and its ligand enhance T-cell growth and dendritic-cell function," Nature, vol. 390, pp. 175-179, 1997.
[5] M. Zaidi, "Skeletal remodeling in health and disease," Nature Medicine, vol. 13, pp. 791-801, Jul 2007.
[6] P. Pivonka, J. Zimak, D. W. Smith, B. S. Gardiner, C. R. Dunstan, N. A. Sims, et al., "Model structure and control of bone remodeling: A theoretical study," Bone, vol. 43, pp. 249-263, 2008.
[7] Yanan Wang, Qing-hua Qin, and S. Kalyanasundaram, "A theoretical model for simulating effect of Parathyroid Hormone on bone metabolism at cellular level," Journal of Molecular & Cellular Biomechanics, vol. 6, pp. 101-112, 2009.
[8] Y. Wang and Q.-H. Qin, "Parametric study of control mechanism of cortical bone remodeling under mechanical stimulus," Acta Mechanica Sinica, vol. 26, pp. 37-44, 2010.
[9] P. Pivonka, J. Zimak, D. W. Smith, B. S. Gardiner, C. R. Dunstan, N. A. Sims, et al., "Theoretical investigation of the role of the RANK-RANKL-OPG system in bone remodeling," Journal of Theoretical Biology, vol. 262, pp. 306-316, 2010.
[10] N. A. Defranoux, C. L. Stokes, D. L. Young, and A. J. Kahn, "In silico modeling and simulation of bone biology: a proposal," J Bone Miner Res, vol. 20, pp. 1079-84, Jul 2005.
[11] A. V. Hill, "The possible effects of the aggregation of the molecules of hemoglobin on its dissociation curves," J. Physiol. (Lond.), vol. 40, 1910.
[12] U. Alon, An Introduction to Systems Biology: Design Principles of Biological Circuits. New York, USA: CRC Press, 2007.
[13] V. Lemaire, F. L. Tobin, L. D. Greller, C. R. Cho, and L. J. Suva, "Modeling the interactions between osteoblast and osteoclast activities in bone remodeling," Journal of Theoretical Biology, vol. 229, pp. 293-309, Aug 7 2004.
[14] G. G. Hannay, D. I. Leavesley, and M. J. Pearcy, "Timing of pulsed electromagnetic field stimulation does not affect the promotion of bone cell development," Bioelectromagnetics, vol. 26, 2005.
[15] J. K.-J. Li, J. C.-A. Lin, H. C. Liu, and W. H.-S. Chang, "Cytokine Release from Osteoblasts in Response to Different Intensities of Pulsed Electromagnetic Field Stimulation," Electromagnetic Biology and Medicine, vol. 26, pp. 153 - 165, 2007.
[16] L.-Y. Sun, D.-K. Hsieh, T.-C. Yu, H.-T. Chiu, S.-F. Lu, G.-H. Luo, et al., "Effect of pulsed electromagnetic field on the proliferation and differentiation potential of human bone marrow mesenchymal stem cells," Bioelectromagnetics, vol. 30, pp. 251-260, 2009.